Macro and meso-scale study in composite lay-up orientation effect on adhesive material used in wind turbine blades

Venkadesh Raman [1], **Monssef Drissi-Habti** [2]

1. *Institut de Recherche Technologique (IRT) Jules Verne,*
   Chemin du Chaffault, 44340 Bouguenais, France
   raman.venkadesh@irt-jules-verne.fr

2. *PRES LUNAM IFSTTAR, CS4 Route de Bouaye, 44344 Bouguenais France,*
   Consortium Durability of Intelligent Composite Structures (GIS DURSI)
   monssef.drissi-habti@ifsttar.fr

ABSTRACT. *Adhesive material is one of the main and fragile component in wind turbine blades. Being large in size compared to the conventional ones, the wind turbine blades are manufactured with composite materials. Generally blades are made by upper and lower sections separately and are joined together by adhesive materials. New generation wind turbines with an increased blade length makes the assembly procedure complicated for the blade manufacturers. Also the adhesive material failure is dependent on the rate of stress transfer between composite and adhesive materials. So, it becomes essential to study the bonding failure both in local and global scale of wind turbine blades. In this paper, we discuss an influence of lay-up orientation of the composite material on the failure of adhesive material used in wind turbine model for macro-scale and single-lap-joint model for meso-scale study.*

RÉSUMÉ. *L'adhésif est l'un des composants principaux et fragiles dans les pales d'éoliennes. Étant de grandes dimensions, les pales d'éoliennes sont fabriquées avec des matériaux composites. En général, les pales sont fabriquées en 2 parties symétriques, qui sont reliées entre elles par du collage. Les nouvelles générations d'éoliennes dotées de dimensions superieures à 100m rend la procédure d'assemblage très compliquée pour les fabricants de pales. La défaillance du matériau adhésif dépend du transfert des contraintes entre les matériaux composites et la colle. Ainsi, il est important d'étudier la défaillance du collage à la fois à l'échelle locale et globale des pales d'éoliennes. Dans cet article, nous abordons l'influence de l'orientation du matériau composite (lay-up) sur la défaillance de matériau adhésif utilisé.*

KEYWORDS: *adhesive bonding, failure, wind turbine blade, composite material, finite element analysis.*

MOTS-CLÉS : *matériau adhésif, défaillance, pale d'éolienne, matériau composite, FEA.*

1. Introduction

Adhesive material is used to assemble the large composite structures. Structural adhesives are specifically formulated to join a variety of high strength composite materials. In wind turbine blades, they are used to bond trailing edge, leading edge and the shear web(s) to the spar caps. The benefits of the structural adhesives are that they are more cleaner, more aerodynamic and visually pleasing compared to the mechanical joints. Adhesive materials for wind turbine applications represent a technical evolution from adhesive formulations developed for other harsh environmental and dynamically-stressed conditions. The geometrical configuration of the bond-lines varies along the blades and it depends mainly on the design of the blade and the manufacturing tolerances. Similar to the matrix in the composite materials, the adhesive joints are expected to transfer the stress from the upper section of the airfoil to the lower section, which are made by composite materials (Cognard, 2006). But, failure initiates mostly at the bond-lines as adhesives are more brittle and fragile compared to the composite materials. Most of the studies focus only on structure reinforcement, but they neglect the end stage structure which includes adhesive bonding. Our aim is to concentrate on adhesive material to provide the knowledge about the critical part of the large structure.

Huang studied the elasto-plastic behavior of adhesive material (Huang, Yang, 2001 ; Yang *et al*., 2004). They explains analytically the bonding behavior by single-lap-joints in elastic and plastic regimes to determine the stress and strain distributions of adhesive-bonded composite.The adhesive was assumed elastic-perfectly plastic and follows von Mises yield criterion. Smeltzer and Tong derived some analytic equations of the adhesive material behavior under bending and shear loads (Smeltzer, Lundgren, 2006 ; Tong, 1996). Their study shows that the peel stress and the shear stress are the main stress components to determine the adhesive behavior. This shear and peel stress behavior would vary consequently, while changing the behavior of the adherend (Leone, 2012 ; Thongchai Fongsamootr, 2005 ; Luo, Tong, 2008 ; Alberto Carpinteri, 2013 ; G.P. Zou, Taheri, 2004 ; Pinto *et al*., 2009). The bonding property changes while they are inserted between dissimilar adherends, because the strain transfer is different based on the modulus of the material (Shahin, Taheri, 2008). Composite material are orthotropic material in which lay-up orientation decides the modulus of material and also the strain transfer properties, this properties cause stress variation in the adjacent structures. Composite material's fiber orientation local effects on adhesives are studied by (Purimpat *et al*., 2013). In our numerical study, we have considered the Single-lap-joint model to concentrate on adhesive material failure properties in order to study the local behavior of bonding. In addition, the same kind of failure study was executed on wind turbine blade model with the purpose of identifying global effect of adhesive material and comparative analysis.

Wind turbine blades are made by composite laminates stacked in the different orientations depending on operating environment. The proper way of blade modeling should be considered for the comparative study. Cox studied the numerical analysis of large scale wind turbines and explained the complexities of large scale design and

aerodynamic behavior (Cox, Echtermeyer, 2013 ; 2012). Meshing and the choice of elements are the main factors to realize the finite element modeling. These properties are clearly studied by (Asseff, Mahfuz, 2009) to avoid the simulation errors. The boundary conditions are very important for the numerical simulation, this load should reflect the maximum effect of wind load acting on the blade (Ashwill, 2010). (Lobitz, P.S.Veers, 1998) studied that the bending and torsion loads are the main forces acting on the blade. He calculated the forces from the aerodynamic forces which is acting in the flap-wise and edge-wise direction. The composite material lay-up arrangement and the thickness should be selected according to the model in order to improve the blade stiffness and rigidity (Zhimin Li, 2013). Ultimately, Gonzlez (Gonzlez *et al.*, 2008) studied bonding effect between blade's sub-component in a small scale experiments. But, the large structures performs different than the small scale structures. In our model, we have referred the details from the above mentioned studies to achieve large scale blade finite element model with bonding lines in the leading edge and trailing edge in order to study the global effect of the adhesive material failure.

Therefore, this paper talk about the meso-scale study was carried-out on a single-lap-joint to identify the failure of bonding material by the combination of different adherends. For macro scale components, the whole blade was simulated in order to find the adhesive material failure from the global effect of blade. The result of numerical simulation will show the adhesive material failure under the comparative study between macro and meso-scale analysis.

2. Analytical method

2.1. Adherend

Although finite element analysis can solve many mechanical problems, analytical solutions are still required to perform parametric analysis. Adherends are composite materials with orthotropic fiber orientation and stress value changes in structure based on the fiber arrangement. The tensor representation of the stress-strain relationship which defines elastic behavior is shown in the equation 1. 'Q' is defined as stiffness matrix.

$$\left(\begin{array}{c} \sigma_1 \\ \sigma_2 \\ \tau_{12} \end{array} \right) = \left(\begin{array}{ccc} Q_{11} & Q_{12} & 0 \\ Q_{21} & G_{22} & 0 \\ 0 & 0 & Q_{66} \end{array} \right) \times \left(\begin{array}{c} \epsilon_1 \\ \epsilon_2 \\ \gamma_{12} \end{array} \right) \tag{1}$$

where, σ and τ are axial and shear stresses, ϵ and γ are axial and shear strains, γ_{12} = Poisson's ratio, $\nu_{12} = \left[\frac{-\epsilon_1}{\epsilon_2} \right]$. In the same way, $\nu_{21} = \left[\frac{-\epsilon_2}{\epsilon_1} \right]$. The stress component in the direction-3 is too low, so σ_3, τ_{31} and τ_{23} values are considered as zero. Q_{11}, Q_{22}, Q_{12} and Q_{66} values are based on Young's modulus and poisson's ratio, see equation 2.

Compliance matrix 'S' is inverted function of the stiffness matrix Q. 'S' gives the strain values of the system according to the applied stress values. Here, S = $Q_{-}1$, ϵ = Sσ.

But this model introduced the shear modulus G_{12} which relates the shear stress to shear strain. E_{11} is longitudinal elastic modulus, E_{22} is transverse elastic modulus.

$$
\begin{pmatrix} \epsilon_1 \\ \epsilon_2 \\ \gamma_{12} \end{pmatrix} = \begin{pmatrix} \frac{1}{E_{11}} & \frac{-\nu_{12}}{E_{11}} & 0 \\ \frac{-\nu_{12}}{E_{11}} & \frac{1}{E_{22}} & 0 \\ 0 & 0 & Q_{66} \end{pmatrix} \times \begin{pmatrix} \sigma_1 \\ \sigma_2 \\ \tau_{12} \end{pmatrix} \tag{2}
$$

The global coordinates of the composite were defined by subscripts x-y. If the fiber is aligned to an angle θ, the local coordinates are defined by 1-2 planes. The coordinate systems are mentioned in the figure 1. The specific orthotropic properties were used to link the global and local coordinate strain values. The 1-2 plane strain values were calculated from the strain values obtained from x-y plan. (x-y directions are load application directions).

$$
\begin{pmatrix} \epsilon_1 \\ \epsilon_2 \\ \gamma_{12} \end{pmatrix} = R \tag{3}
$$

$$
\begin{pmatrix} \epsilon_1 \\ \epsilon_2 \\ \frac{\gamma_{12}}{2} \end{pmatrix} = R.T. \begin{pmatrix} \epsilon_x \\ \epsilon_y \\ \frac{\gamma_{xy}}{2} \end{pmatrix} \tag{4}
$$

$$
R.T.R^{-1} = \begin{pmatrix} \epsilon_x \\ \epsilon_y \\ \gamma_{xy} \end{pmatrix} \tag{5}
$$

Where,

$$
R = \begin{pmatrix} 1 & 0 & 0 \\ 0 & 1 & 0 \\ 0 & 0 & 2 \end{pmatrix} \tag{6}
$$

$$
T = \begin{pmatrix} cos^2\theta & sin^2\theta & 2sin\theta cos\theta \\ sin^2\theta & cos^2\theta & {}_2sin\theta cos\theta \\ -sin\theta cos\theta & sin\theta cos\theta & cos^2\theta - sin^2 theta \end{pmatrix} \tag{7}
$$

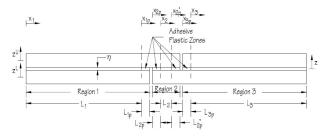After several derivations, the equation can be reduced to

$$
\begin{pmatrix} \sigma_x \\ \sigma_y \\ \tau_{xy} \end{pmatrix} = T^{-1}.Q.R.T.R^{-1} \begin{pmatrix} \epsilon_x \\ \epsilon_y \\ \gamma_{xy} \end{pmatrix} \tag{8}
$$

From equations 7 and 8, we observed that the stress values in the load direction is based on the value θ in the matrix T. Therefore, alignment of fiber have an important role of stress distribution. This stress distribution may cause variations in failure values in the meso and macro scale models.

2.2. Adhesive

The composite adherends were assumed to be linear-elastic while the adhesive was assumed as elastic-perfectly plastic following von Mises yield criterion (Yang *et al.*, 2004). The entire coupled system was then determined through the kinematics and force equilibrium of the adhesive and the adherends. Major failure modes of adhesive-bonded joints are (1) cohesive failure, (2) adhesive failure, and (3) adherend failure.The wind turbine blade joints are pertaining to adhesive layer. Therefore, focus of this current study is on adhesive failure mode.

First order plate theory was used to determine the properties of top and bottom adherends. Displacement fields in the peel and shear direction are represented by w and u (see figure 2)- can be written as

Source: (Yang *et al.*, 2004)

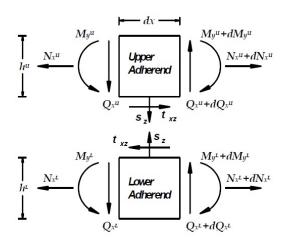*Figure 1. Single-lap-joint configurations and coordinate systems*

$$u^U = u^{O\,U(x)} + Z^U \psi^U(x) \tag{9}$$

$$u^L = u^{O\,L(x)} + Z^L \psi^L(x) \tag{10}$$

$$w^U = w^U(x) \tag{11}$$

$$w^L = w^L(x) \tag{12}$$

$_0$ and ψ represent mid-plane displacement and bending slops respectively. U and L correspond to upper and lower adherends respectively. By substituting the equations

Source: (Yang *et al.*, 2004)

Figure 2. Single lap-joint free body diagram

(9) - (12) to the strain-displacement relation together with the matrices of equivalent modulus [A], [B], and [D] for orthotropic laminate, also normal stress N_x, bending moment M_y and resultant transverse shear stress Q_z can be obtained as,

$$N_x = A_{11}\frac{du^o(x)}{dx} + B_{11}\frac{d\psi(x)}{dx} \tag{13}$$

$$M_y = B_{11}\frac{du^o(x)}{dx} + D_{11}\frac{d\psi(x)}{dx} \tag{14}$$

$$Q_z = kA_{55}\left(\psi(x) + \frac{dw(x)}{dx}\right) \tag{15}$$

From figure 2, the equilibrium equation was established for single-lap-joint. While calculating resulting forces,

$$\frac{dN_x^U}{dx} = -\tau_{xz} \tag{16}$$

$$\frac{dM_y^U}{dx} = Q_z^U + \frac{h^U}{2}\tau_{xz} \tag{17}$$

$$\frac{dQ^U}{dx} = \sigma_z \tag{18}$$

where,

(i) τ_{xz}= shear stress

(ii) σ_z = peel stress

(ii) h^U = adherend thickness.

Equilibrium equation for the lower adherend was derived in a same way. Adhesive behavior was derived for elastic and plastic regions separately. By assuming a perfect bonding between the adherends and adhesive material, the adhesive deformation and strain are based on the bottom surface of the top adherend and the top surface of the bottom adherend as seen in figure 2, in other words, contact zones. In terms of field displacement of two laminates, the adhesive strains are,

$$\gamma_{xz} = \frac{\left((u^{oL} - u^{oU}) + (\frac{h^L}{2}\psi^L + \frac{h^U}{2}\psi^U) - (\frac{dw^L}{dx} + \frac{dw^U}{dx})\right)}{\eta} \tag{19}$$

$$\epsilon_x = \frac{1}{2}\left(u^{oL} + u^{oU}\right) + (\frac{h^L}{2}\psi^L - \frac{h^U}{2}\psi^U) \tag{20}$$

$$\epsilon_z = \frac{1}{2}(w^U - w^L) \tag{21}$$

Based on above terms, we can derive the stress components in 3 directions of adhesive,

$$\sigma_x = \frac{E}{(1+\nu)(1-2\nu)}\Big[(1-\nu)\epsilon_x + \nu\epsilon_z\Big] \tag{22}$$

$$\sigma_z = \frac{E}{(1+\nu)(1-2\nu)}\Big[\nu\epsilon_x + (1-\nu)\epsilon_z\Big] \tag{23}$$

$$\tau_{xz} = G\gamma_{xz} \tag{24}$$

Adhesive yielding occurs in the edges of the adhesive layer, therefore plastic behavior was assumed in these edges. The stress components in the x, y and z directions are similar to the equations derived in elastic behavior. But, the shear property values are much higher than deviotric stresses $(\sigma_x, \sigma_y and \sigma_z)$. Yield stress is calculated by Von Mises yield criterion based on Prandlt - Reuss material model [15].

$$\sigma' = \sqrt{\frac{3}{2}(S_x^2 + S_y^2 + S_z^2) + \tau_{xz}^2} \tag{25}$$

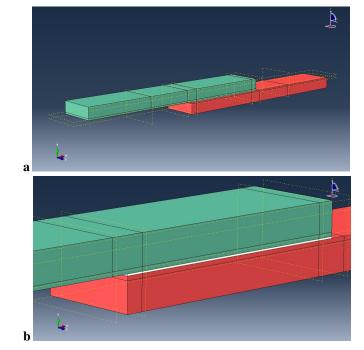$$\tau_{xz} = \tau_p = \frac{\sigma_{yield}}{\sqrt{3}} \tag{26}$$

Where, $S_x, S_y and S_z$ are the function of plastic potential g,

$$g = \frac{1}{2}S_{ij}S_{ji} \tag{27}$$

Plastic behavior of adhesive material in signal-lap-joint shows that the stress concentration values are dependent on the shear stress value and it is approximately proportional to the maximum stress value, see equation 26. Also, these equations provide an illusion of the material failure modes and the influences of stresses during the finite element model calculation based on composite material orientation. The strain energy release rate was observed in the adhesive zone in order to find out the deformation rate around the contact zone.

3. Numerical analysis

3.1. Meso-scale Model

Figure 3. (a) Single-lap-joint Numerical model, (b) Single-lap-joint Numerical model zoomed(white color part represents the adhesive layer)

Meso-scale study of adhesive material deformation was performed in single-lap-joint. The load was applied at top adherends as traction forces in outward direction from side-surface and the bottom adhered is fixed at the end. Both adherends were considered orthotropic, the adhesive was considered as isotropic material and its properties are not depending on any direction orientation. The adherends were assumed to act as linear elastic cylindrical bend plates under plain strain conditions.
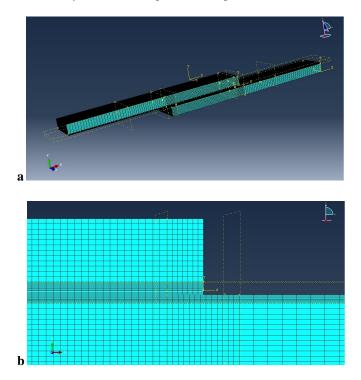

Figure 4. (a) Single lap-joint mesh, (b) Mesh around the adhesive joints

Single-lap-joint model was designed in adaqus/standard software. The adherends modeled with 70 mm length, 12mm width and 4mm thickness. Effective length of adhesive layer was designed with 30 mm between two adherends and consist 0.2 mm thickness. The adhesive material elements are defined as solid elements. The composite material contains quadratic plane stress elements. The entire model inheres 13,61,200 elements. The composite material was composed 8 plies in which 0.5mm is a single ply thickness. Top and bottom adherends were defined as composite material (see figure 3). The green and red color components are composite adherends and the thin white layer represents bonding. The model was meshed with elements as defined above, the dense mesh zone indicates adhesive material (figure 4). Orthotropic composite material and isotropic adhesive material were linked by nodal contact. This study concentrated on mode 2 or sliding mode, as bonding of wind turbine blade's skin is more concerned by shear properties. The bottom adherend was fixed at the free

end, but top adherend undergoes traction force of 400N, this provided shear and peel stress concentrations at the adhesive material. As adhesive material study was accomplished uniquely for skin of the blade, the blade material properties were defined only with woven fabrics type composite material, because the previous result showed that the skins are made of glass or carbon woven composites. Different ply orientations of these composite material and their effects on adhesive material were analyzed.

3.2. Meso-scale result

The composite lay-up orientation plays a vital role in transferring the strain energy from bottom to top adherend which results the change in mechanical behavior of structure (Eq.(27)). The failure at the adhesive material is shown in different views in figure 5.
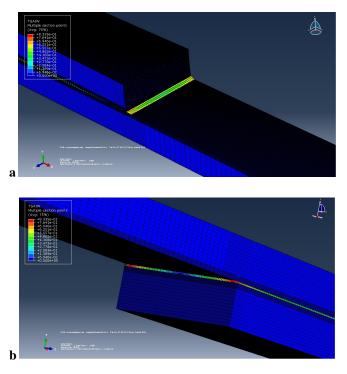

Figure 5. (a) Tsai-wu failure in single lap joint close to bottom adherend, (b) Tsai-wu failure in single-lap-joint close to top adherend

In the strain energy curves, we can observe that the initial strain energy release value increases gradually from cross, multi and angle plies for bi-materials and accordingly strain values observed from the displacement rate corresponds to the strain energy curve, figures 6, 7, 8. The carbon angle ply adherends released maximum strain energy under mode-2 in the adhesive contact zone (see figure 8).
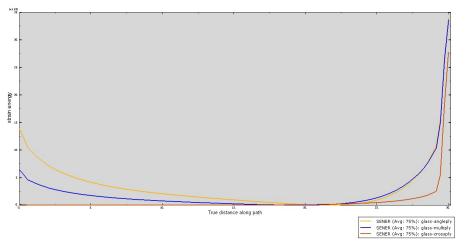
Figure 6. Strain energy release in glass fiber composites, x axis - effective length(mm), y axis - strain energy($\times 10^3$)
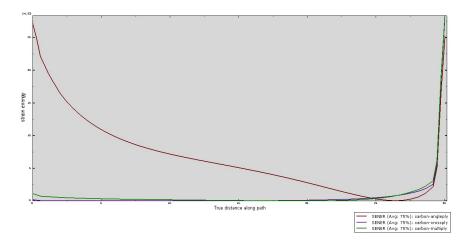

Figure 7. Strain energy release in carbon fiber composites, x axis -effective length(mm), y axis -strain energy($\times 10^3$)
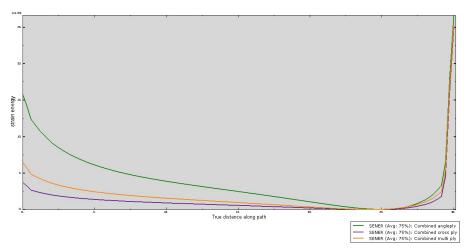
Figure 8. Strain energy release in glass-carbon fiber composites, x axis - effective length(mm), y axis - strain energy($\times 10^3$)

3.3. Macro scale model

It is imperative to compare the local adhesive behavior with global effect of adhesive by studying large scale wind turbine model. In our model, the blade was designed by shell element with skins and spars by using abaqus software (Cox, Echtermeyer, 2013). The blade length is 70m and the chord length at the root is equal to 3m. The chord length at the tip was considered to be 1.5m. The blade had a twist angle throughout the span. This twist angle was assumed to be 15° from root to tip. The following figure 9 shows the designed aerodynamic configurations and the final model of the blade in the Abaqus user interface. The blade was meshed with quadratic shell elements, and some complex surfaces are meshed with triangular shell elements to avoid the hourglass effect of meshes (see figure 10), the complete blade contains 2323888 elements.
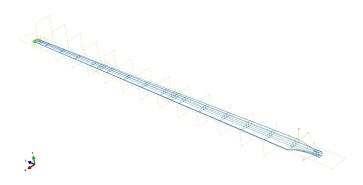

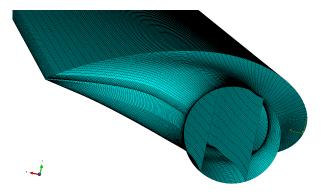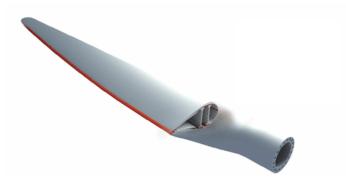*Figure 9. Blade geometrical model designed in abaqus*

Figure 10. Meshed blade model with shell elements

Type of fabrics should be selected based on the application and load direction. Unidirectional tapes and woven fabrics were analyzed in the previous study, and the woven fabrics were found more suitable for wind turbine blade skin. Bending load was applied at 3 points a, b, c which are located in range of 2m, 20m and 45m gradually from the blade tip. Calculations were carried out at a wind speed of 15m/s by blade element momentum theory, that provides a 150KN bending force distributed in 3-points (26.6 KN at point a, 33.5 KN at point b, 40 KN at point c) and 200KNm twisting moment at shear center of blade tip chord section (Lobitz, P.S.Veers, 1998). The adhesive zone was defined at both the leading and trailing edges of the blade as shown in the figure 11. In this simulation, we used Macroplast U1345 type adhesive material which is commonly used on wind-turbine application (sheet, s. d.). The adhesive material thickness was 4mm in the numerical simulation model.

Source: (sheet, s. d.)

Figure 11. Bonding zones(red color)in wind turbine blade

The blade was designed with glass/vinyl-ester (GFRP) woven fabrics or carbon epoxy (CFRP) woven fabrics composite materials (Conshohocken, 2002). The Angle, cross and multi-plies were used to define the blade material, see table 1. Each plies

describe different shear and principal stress in different location of blades. Blade components are bonded as shown in the figure 11 and these adhesive materials were introduced in the numerical model.

Tableau 1. Mechanical properties of composite material

$Materials$	$E_1(GPa)$	$E_2(GPa)$	ν_{12}	$G_{12}(GPa)$	$G_{23}(GPa)$
$Woven fabric - Gl$	23.37	23.50	0.28	5.22	4.74
$Woven fabric - Ca$	63	62.73	0.05	4.37	2.91

Failure of adhesive material was analyzed by Tsai-wu failure criterion under isotropic material condition. Tsai-wu value less than 1 represents the failure value within a safety limit. For both cases the failure values were observed only in adhesive material.

3.4. Macro-scale results

The blade was simulated in static bending and torsion loading conditions (Lobitz, P.S.Veers, 1998). Figure 12 shows that the failure took place close to root section and the adhesive material in trailing edges. The trailing edge failure is caused due to the presence of adhesive material experiencing the torsion load applied at the shear center. This zone was more affected by shear stress. The adhesive materials were normally experiencing failure prior to the composite material.
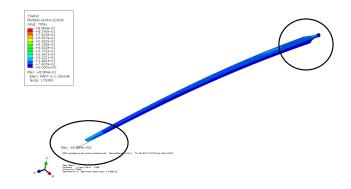

Figure 12. Failure at trailing edge and root section of wind turbine, maximum tsai-wu value is observed in trailing edge

4. Discussions

For meso scale model, figure 13a indicates that the cross ply carbon woven composite adherends provide large peel stress and failure accompanied by less displacement (figure 14b). This property is based on the stiffness of the adherends. Therefore, adherends with high stiffness would lead to low strain value and vice versa. S_{22} reflects the

shear stress of the adhesive (locally) and longitudinal stress of adherend, as the load applied on single-lap-joint provides shear stress(mode-2) to the adhesive and S_{12} provides pure shear stress. Here, displacement represents the top adherend's peel distance (Quaresimin, Ricotta, 2006).
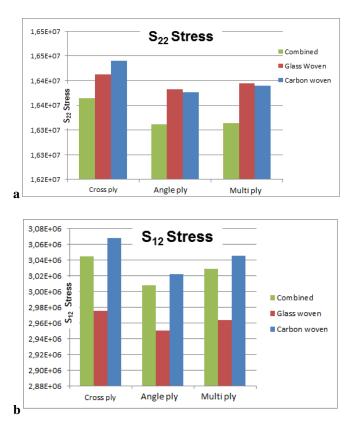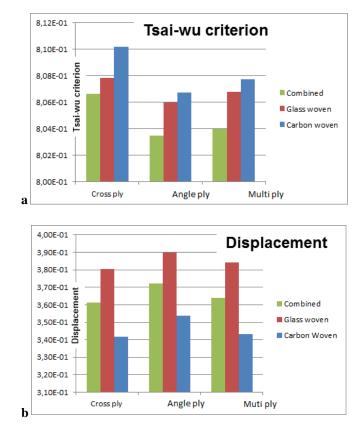

Figure 13. (a) S_{22} stress observed in single-lap-joint (y axis-$S_{22}, N/m^2$), (b) S_{12} stress observed in single-lap-joint (y axis-$S_{12}, N/m^2$)

Pure shear stress values S_{12} for glass fiber composites were low for all orientations (figure 13b), because of good shear resistance priovided by glass fibers. On the contrary, displacement values were high. The displacement values obtained from the glass angle-ply adherends were higher compared to that of carbon angle-ply adherends but its S_{12} and failure values were low. So we could assume that the angle ply orientation of GFRP provides good rigidity in adhesive zone. On the other hand, the CFRP adherend at bottom and GFRP adherend on top (hereby called bi-material joint) allocates less S_{22} stress (Saleh et al., 2015). This bi-material provide less peeling stress, S_{22} that leads to low failure value, see figure 14a. Therefore, the peel stress had major influence on failure value calculations. These results also show that the *adherend's*

Figure 14. (a) Tsai-wu value in single-lap-joint (y axis-Tsai-wu value), (b) displacement value in single lap joint (y axis-Displacement,mm)

orientation with multi-ply and angle ply orientations are efficient for joining different FRPs.

Bi-material adherend bonding might provide high displacement compared to CFRP, but the cost analysis study shows that the simple CFRP is costlier than bi-material adherends (Das, 2001). Thus, it is observed that using bi-material joint in multi-ply orientation is advantageous. Carbon cross ply and bi-material adherends in multi-ply provides 10% variation in adhesive failure criterion.

In macroscale model, table 2 shows the failure values at 344456 elements for all composite material orientations (see figure 15). For carbon fiber blade, multi-ply orientation provides less failure in bonding and maximum failure value was noted in angle ply configuration. Whereas for the glass fiber blade, angle ply configuration gave less failure value. In view of the facts, shear strength is higher for glass fiber composites in angle ply orientation method.

Glass-fiber multi-ply configuration provides failure value in-between the failure value of angle and cross ply with the same material property. It proves that the failure values are based on ply orientation, although the same material was used (table 2). Carbon multi-ply reduces 27% in failure value compared to carbon angle ply and also reduce 13% compare to glass angle plies. This result can help and furnish the knowledge to large scale rotor designers to select the proper adhesive material property in order to avoid the failure, while the ply orientation changes for the same material in use.
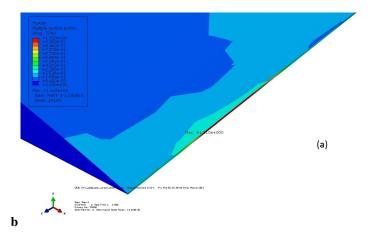

Figure 15. Trailing edge adhesive material failure

Tableau 2. Tsai-wu value of adhesive material used in macro scale analysis.

$Material$	$Ca)a.ply$	$Ca)c.ply$	$Ca)m.ply$	$Gl)a.ply$	$Gl)c.ply$	$Gl)m.ply$
$TsaiWu$	0.996	0.8681	0.7259	0.8344	0.9079	0.8626

(i) Ca - Carbon woven composite material(CFRP)

(ii) Gl - Glass woven composite material(GFRP)

(iii) *c.ply - Cross ply - 0°/90°

(iv) *a.ply - Angle ply - 45°/-45°

(v) *m.ply - Multi ply - 0°/90°/45°/-45°

In meso model, the carbon angle ply adherends released maximum strain energy under mode-2 in the adhesive contact zone (see figure 8), same configuration gave maximum failure values which was caused by torsional force compared to other configurations at macro-scale model (see table 2). And also multi-ply orientation is providing minimum failure value based on Tsai-wu factor and cost study for both approaches. Therefore, meso-scale analysis was completely reflected in the macro scale simulation. These proved that the local adhesive failure study is essential and effective to collect the basic adhesive properties for large scale structures.

5. Conclusion

Failure in adhesive material was studied in macro and meso scale level. In both cases, the simulation was accomplished under quasi-static load condition. From the macro study, CFRP adherend in multi-ply orientation and GFRP adherend in angle ply provided minimum failure. But in the meso-scale study, it is obsereved that the failure values obtained by multi-ply and angle ply orientations were similar and the strain values for multi-ply were close to that of the cross-ply configuration. In macro scale model, a big difference in failure criterion was observed between the glass and carbon angle ply configurations, which was also identified in the meso scale strain energy release rate curve. Both the approaches showed that the multi-ply orientation provided less failure for the adhesive material. Therefore, this study clearly shows that the adhesive material failure varies when designed lay-up orientation changes in both meso and macro scale structure. Also we have proven that the macro-scale structure failure follows the same material behavior at meso-scale. This study also could provide preliminary knowledge of adhesive bonding based on failure for various lay-ups at different scale applications, especially for wind turbine blades.

Bibliography

Alberto Carpinteri M. P. (2013). Influence of the interface bonding strength on brittle crack propagation in bi-material structural components. *15th European Conference on Fracture (ECF)*. (T Technology > TJ Mechanical engineering and machinery)

Ashwill T. D. (2010). Passive load control for large wind turbines. *American Institute of Aeronautics and Astronautics*, n° SAND2010-3276C.

Asseff N. S., Mahfuz H. (2009, Oct). Design and finite element analysis of an ocean current turbine blade. In *Oceans 2009*, p. 1-6.

Cognard J. (2006). Some recent progress in adhesion technology and science. *Comptes Rendus Chimie*, vol. 9, n° 1, p. 13 - 24. (Adhesion Adhesion)

Conshohocken W. (2002). *Composite materials handbook* (vol. 2). Department of defense. (Polymer matrix composite materials properties)

Cox K., Echtermeyer A. (2012). Structural design and analysis of a 10mw wind turbine blade. *Energy Procedia*, vol. 24, p. 194 - 201. (Selected papers from Deep Sea Offshore Wind Ramp;D Conference, Trondheim, Norway, 19-20 January 2012)

Cox K., Echtermeyer A. (2013). Geometric scaling effects of bend-twist coupling in rotor blades. *Energy Procedia*, vol. 35, p. 2 - 11. (DeepWind'2013 - Selected papers from 10th Deep Sea Offshore Wind Ramp D Conference)

Das S. (2001). The cost of automotive polymer composites:a review and assessment of doe's lightweight materials composites research. *Energy dicision, Oak Ridge National Laboratory*.

Gonzlez A. C., Bussel G. van, Nijssen R. (2008). *Evaluation of bondline thickness on wind turbine blade subcomponents*. Mémoire de Master non publié, Eindhoven:Technische Universiteit Eindhoven. (Master sustainable energy technology)

G.P. Zou K. S., Taheri F. (2004). An analytical solution for the analysis of symmetric composite adhesively bonded joints. *Composite Structures*, vol. 65, n° 3-4, p. 499 - 510.

Huang H., Yang C. (2001). Elastic-plastic model of adhesive-bonded composite joints. *13th international conference on composite materials*.

Leone D. C. G., Frank A.Jr. Girolamo Donato. (2012). Progressive damage analysis of bonded composite joints. *Technical Report, NASA/TM-2012-217790, L-20210, NF1676L-15757*.

Lobitz D., P.S.Veers. (1998). Aeroelastic behavior of twist-coupled hawt blades. *American Institute of Aeronautics and Astronautics*.

Luo Q., Tong L. (2008). Analytical solutions for adhesive composite joints considering large deflection and transverse shear deformation in adherends. *International Journal of Solids and Structures*, vol. 45, n° 22-23, p. 5914 - 5935.

Pinto A. M. G., Magalhaes A. G., Campilho R. D. S. G., Moura M. F. S. F. de, Baptista A. P. M. (2009). Single-lap joints of similar and dissimilar adherends bonded with an acrylic adhesive. *Journal of Adhesion*, vol. 85, p. 351–376.

Purimpat S., Jerome R., Shahram A. (2013). Effect of fiber angle orientation on a laminated composite single-lap adhesive joint. *Advanced Composite Materials*, vol. 22, n° 3, p. 139-149.

Quaresimin M., Ricotta M. (2006). Stress intensity factors and strain energy release rates in single lap bonded joints in composite materials. *Composites Science and Technology*, vol. 66, n° 5, p. 647 - 656. (Reliability and Life Prediction of Composite Structures9th European-Japanese Symposium on Composite Materials)

Saleh P., Challita G., Khalil K. (2015). Stress concentration coefficient in a composite double lap adhesively bonded joint. *International Journal of Adhesion and Adhesives*, vol. 63, p. 102 - 107.

Shahin K., Taheri F. (2008). The strain energy release rates in adhesively bonded balanced and unbalanced specimens and lap joints. *International Journal of Solids and Structures*, vol. 45, n° 25-26, p. 6284 - 6300.

sheet T. data. (s. d.). *Macroplast uk 1340-b90*.

Smeltzer S., Lundgren E. (2006). Analytical and numerical results for an adhesively bonded joint subjected to pure bending. *47th AIAA/ASME/ASCE/AHS/ASC Structures, Structural Dynamics, and Materials Conference*.

Thongchai Fongsamootr C. D. (2005). Stress analysis of thin adhesive bonding dissimilar adherends single lap joints. *11th International conference on Fractur*.

Tong L. (1996). Bond strength for adhesive-bonded single-lap joints. *Acta Mechanica*, vol. 117, n° 1, p. 101–113.

Yang C., Huang H., Tomblin J. S., Sun W. (2004). Elastic-plastic model of adhesive-bonded single-lap composite joints. *Journal of Composite Materials*, vol. 38, nº 4, p. 293-309.

Zhimin Li C. L. (2013). Effect of layup design on properties of wind turbine blade. *Frontiers of Engineering Mechanics Research*, vol. 2, p. 63-70.